


Formation of the Little Red Dots from the Core-collapse of Self-interacting Dark Matter Halos

FANGZHOU JIANG ^{1,*} ZIXIANG JIA,² HAONAN ZHENG,¹ LUIS C. HO,^{1,2} KOHEI INAYOSHI,¹ XUEJIAN SHEN,^{3,4}
MARK VOGELSBERGER,⁴ AND WEI-XIANG FENG⁵

¹*Kavli Institute for Astronomy and Astrophysics, Peking University, Beijing 100871, China*

²*Department of Astronomy, School of Physics, Peking University, 5 Yiheyuan Road, Beijing, 100871, China*

³*Department of Physics, Massachusetts Institute of Technology, Cambridge, 02139, MA, USA*

⁴*Kavli Institute for Astrophysics and Space Research, Massachusetts Institute of Technology, Cambridge, 02139, MA, USA*

⁵*Department of Physics, Tsinghua University, Beijing 100084, China*

ABSTRACT

We present a statistical study on the formation and growth of black holes (BHs) seeded by gravothermal core-collapse of self-interacting dark matter (SIDM) halos at high redshifts, using a semi-analytical framework based on Monte-Carlo merger trees. We demonstrate that BH formation via gravothermal collapse naturally occurs in high-concentration halos at a characteristic mass scale determined by the SIDM cross section, and only during the early Universe. This mechanism is particularly promising for explaining the abundance of little red dots (LRDs) — a population of early, apparently galaxy-less active galactic nuclei hosting supermassive BHs. By incorporating this seeding process with simplified models of BH growth and mergers, we successfully reproduce the observed LRD mass function for moderately large cross sections of $\sigma_{0m} \sim 30 \text{ cm}^2 \text{ g}^{-1}$ and $\omega \sim 80 \text{ km s}^{-1}$, intriguingly consistent with independent local constraints derived from galaxy rotation curves. Our results highlight the potential of high-redshift BH statistics as a complementary probe for constraining SIDM models.

Keywords: Dark matter(353) — Supermassive black holes(1663) — Galaxy dark matter halos(1880)
— Early universe(435)

1. INTRODUCTION

Self-interacting dark matter (SIDM) has emerged as an appealing candidate to address longstanding cosmological challenges (Weinberg et al. 2015; Sales et al. 2022). Unlike the standard cold dark matter (CDM) model, SIDM introduces elastic scattering between dark matter (DM) particles, preserving CDM’s successes on large scales (e.g., Rocha et al. 2013; Despali et al. 2025) while significantly altering halo structures on smaller scales. These alterations manifest primarily in two phases driven by gravothermal evolution: first, the formation of an isothermal core that can potentially resolve the cusp-core discrepancy observed in dwarf galaxy rotation curves without invoking baryonic physics (Spergel & Steinhardt 2000; Kaplinghat et al. 2014, 2016); second, a gravothermal instability leading to core-collapse and the eventual formation of central black holes (BHs) (Balberg & Shapiro 2002; Pollack et al. 2015).

Recent theoretical advancements highlight SIDM core-collapse as a promising mechanism for seeding supermassive black holes (SMBHs) in the early Universe. Feng et al. (2021, 2022) show via relativistic calculations that about 0.1-1% of halo mass will turn into a BH seed, independent of the mass or structure of the halo at formation. Roberts et al. (2025) indicates that rare, massive SIDM halos at high redshifts ($z \sim 6-10$) can rapidly collapse to form seed BHs as massive as $\sim 10^7-10^9 M_\odot$, potentially explaining the existence of extremely massive quasars at cosmic dawn. However, beyond these extreme systems, a more pervasive observational challenge has emerged with the discovery of little red dots (LRDs) — a new population of compact, high-redshift ($z \gtrsim 5$) active galactic nuclei that appear unusually abundant (Kokorev et al. 2024; Kocevski et al. 2024; Maiolino et al. 2024) yet remarkably deficient in stellar components (Chen et al. 2024). These enigmatic systems, likely hosting SMBHs with masses ranging from 10^6 to $10^8 M_\odot$ (Matthee et al. 2024; Greene et al. 2024; Taylor et al. 2024), pose significant challenges to traditional baryonic seeding scenarios (Inayoshi et al. 2020;

* Corresponding author: fangzhou.jiang@pku.edu.cn
Boya Young Fellow

Volonteri et al. 2021) and conventional galaxy-BH co-evolution pictures (Kormendy & Ho 2013; Reines & Volonteri 2015).

It is thus interesting to explore the possibility that LRDs originate from DM via SIDM core-collapse. If core-collapse occurs prior to re-ionization, BHs can form in halos that are devoid of significant stellar components. The critical question then arises: what conditions must be met for this dark seeding mechanism to take place? Qualitatively, core-collapse must occur early enough, while the DM halos responsible for seeding these BHs must be sufficiently massive to account for the observed BH masses. These two conditions are in competition due to the hierarchical nature of structure formation. Furthermore, the timing of core-collapse is intricately linked to the cross section of dark self-scattering, as the cross section, along with halo mass and structure at formation, determines the timescale for core-collapse (Balberg & Shapiro 2002; Pollack et al. 2015; Yang et al. 2023).

In this Letter, we present a proof-of-concept study addressing this question. In Section 2, we demonstrate the existence of a characteristic halo mass scale at which SIDM core-collapse occurs most rapidly. In Section 3, we further clarify the conditions required for BH seeding, exploring which halos can collapse sufficiently early to explain the observed properties of LRDs. We introduce a semi-analytic framework for modeling BH seeding and subsequent growth in Section 4. Using this model, we compute the predicted BH mass function in Section 5, illustrating that SIDM scenarios can naturally reproduce the observed LRD populations. Finally, in Section 6, we discuss how the SIDM cross section accommodating the LRD population relates to completely independent constraints from galaxy kinematics, and we summarize our finding in Section 7.

Throughout this study, we define the virial radius of a DM halo as the radius enclosing an average density equal to 200 times the critical density of the Universe. We adopt a flat cosmological model characterized by the present-day matter density $\Omega_m = 0.3$, baryonic density $\Omega_b = 0.0465$, dark-energy density $\Omega_\Lambda = 0.7$, power-spectrum normalization $\sigma_8 = 0.8$, spectral index $n_s = 1$, and a Hubble parameter $h = 0.7$. Following standard convention, we express the DM self-interaction cross section in terms of the cross section per unit particle mass, $\sigma_m = \sigma/m_\chi$, where m_χ is the mass of a DM particle. We consider velocity-dependent cross sections specified by two parameters, a low-velocity cross section σ_{0m} and a characteristic velocity scale ω , above which cross section rapidly declines (Yang & Yu 2022).

2. CHARACTERISTIC HALO MASS FOR FASTEST CORE-COLLAPSE

To seed a BH from an SIDM halo at high redshift, the characteristic timescale for gravothermal core-collapse must be very short. Since this timescale is sensitive to the self-interaction cross section, we first clarify our definition of the DM scattering cross section before elaborating on the core-collapse time.

Consider an SIDM particle χ coupled to a light gauge boson ϕ . In the perturbative (Born) regime, the differential cross section for elastic self-scattering in the center-of-momentum frame, assuming Rutherford-type scattering, is given by (Yang & Yu 2022):

$$\frac{d\sigma}{d\cos\theta} = \frac{\sigma_0\omega^4}{2[\omega^2 + v^2 \sin^2(\theta/2)]^2} \quad (1)$$

where $\sigma_0 = 4\pi\alpha_\chi^2/(m_\chi^2\omega^4)$ is the low-velocity limit of the cross section, α_χ is the coupling strength, $\omega = m_\phi c/m_\chi$ is the velocity scale above which cross section sharply declines, θ is the scattering angle, and v is the relative velocity between two DM particles.

For an SIDM halo, it is useful to define an effective, velocity-averaged cross section by integrating the velocity-dependent cross section over the velocity distribution (Yang & Yu 2022; Yang et al. 2023):

$$\sigma_{\text{eff}} = \frac{1}{2} \int \tilde{v}^2 d\tilde{v} \sin^2\theta d\cos\theta \frac{d\sigma}{d\cos\theta} \tilde{v}^5 e^{-\tilde{v}^2}, \quad (2)$$

where $\tilde{v} \equiv v/(2v_{\text{eff}})$, and v_{eff} is a characteristic one-dimensional velocity dispersion. For an isotropic velocity field, it can be approximated by $v_{\text{eff}} \approx v_{\text{max}}/\sqrt{3}$, with v_{max} being the maximum circular velocity of the halo.

Following previous studies (Balberg & Shapiro 2002; Pollack et al. 2015; Essig et al. 2019; Yang et al. 2023), we approximate the core-collapse time as:

$$t_{\text{cc}} \approx \frac{150}{C} \frac{1}{\sigma_{\text{eff},m}\rho_s r_s} \frac{1}{\sqrt{4\pi G\rho_s}}, \quad (3)$$

where C is an empirical constant calibrated with N -body simulations, for which we adopt $C = 0.75$, consistent with Nishikawa et al. (2020)¹, and $\sigma_{\text{eff},m}$ is the effective cross section per particle mass. This expression implies that the lifetime of the halo core prior to collapse is a multiple of the collisional relaxation time, which scales as $(G\rho_s)^{-1/2}$, evaluated at the time of halo formation. We assume the halo follows a Navarro, Frenk

¹ This fudge factor, of order unity, is related to the thermal conductivity of the gravothermal fluid and may depend on the detailed structure of the halo.

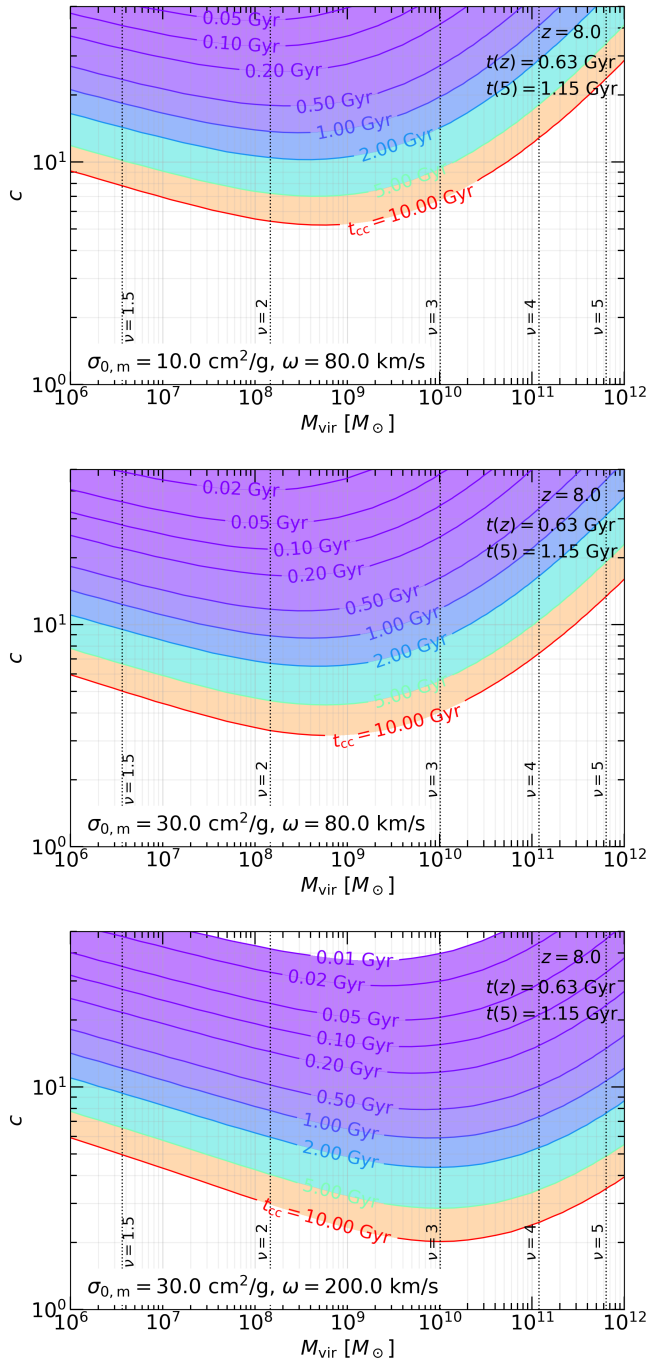


Figure 1. Contours of SIDM core-collapse timescale t_{cc} as a function of halo concentration c and halo mass M_{vir} at redshift $z = 8$. Cross sections are indicated in the lower-left corners. Cosmic times at $z = 8$ and $z = 5$ are labeled in the upper-right corners. Halos located above a given contour, $t_{cc} \lesssim (1.15 - 0.63) \text{ Gyr} \approx 0.5 \text{ Gyr}$, can undergo core-collapse by the time of $z = 5$, representative of LRDs. Clearly, timely core-collapse requires halos with high concentrations ($c \sim 10$). Vertical dotted lines indicate halo rarity in terms of their density peak height ν . The characteristic halo mass corresponding to the fastest core-collapse aligns with rare 2-3 σ peaks, shifting to higher masses with increasing effective cross section (top to bottom panels).

& White (NFW) profile (Navarro et al. 1997) at the time of formation:

$$\rho(r) = \frac{\rho_s}{r/r_s(1+r/r_s)^2}, \quad (4)$$

where ρ_s and r_s are the scale density and scale radius, respectively. An NFW halo can be fully specified by these two parameters, or equivalently by its virial mass M_{vir} and concentration parameter $c \equiv r_{\text{vir}}/r_s$, where r_{vir} is the virial radius. These are related through:

$$M_{\text{vir}} = 4\pi\rho_s r_s^3 f(c) \quad (5)$$

and

$$\rho_s = \frac{c^3}{3f(c)} \Delta\rho_{\text{crit}}(z), \quad (6)$$

with $f(x) = \ln(1+x) - x/(1+x)$, $\Delta = 200$, and $\rho_{\text{crit}}(z)$ the critical density of the Universe at redshift z . To leverage established theoretical models describing the evolution of halo virial mass (e.g., Lacey & Cole 1993), we use M_{vir} and c to define the NFW profile of the halo at its formation epoch.

From eqs. (3)-(6), it is clear that the core-collapse timescale decreases with increasing halo concentration and self-interaction cross section. Less obvious, however, is a non-monotonic dependence on halo mass. Fig. 1 illustrates these trends, showing contours of t_{cc} in the parameter space defined by halo concentration c and virial mass M_{vir} . For illustrative purposes, we consider a scenario where halo virialization occurs at $z \sim 8$. We also consider a reference redshift of $z = 5$, typical for LRDs, so the time interval is $\sim 0.5 \text{ Gyr}$. Several insights into BH seeding conditions emerge from this figure.

First, a very high halo concentration — at least $\gtrsim 10$ — is required for the core-collapse time to fall below $\sim 0.5 \text{ Gyr}$. If gravothermal evolution begins at $z = 8$ such a collapse timescale would bring the system to $z \sim 5$, just early enough for the resulting BH to be observed as an LRD. While the average halo concentration at these redshifts is typically ~ 3 (e.g., Yung et al. 2024), concentrations as high as $c \sim 10$ is still attainable, as we will discuss shortly.

Second, for a fixed cross section and concentration, there exists a characteristic halo mass at which core-collapse is most efficient. If the halo mass is significantly below this characteristic value, the central density is too low for effective self-scattering. Conversely, if the mass is too high, the cross section becomes too small due to the strong velocity dependence described in eq. (1). Interestingly, for the cross-section range explored here ($\sigma_{0m} \sim 10\text{-}30 \text{ cm}^2 \text{ g}^{-1}$, $\omega \sim 80\text{-}200 \text{ km/s}$), this characteristic mass lies in the range $M_{\text{vir}} \sim 10^8\text{-}10^{10} M_{\odot}$ — assuming that roughly 1% of the halo mass ends up in the

BH (Feng et al. 2021), this yields seed BH masses of $M_{\text{bh}} \sim 10^{6-8} M_{\odot}$, already comparable to those powering LRDs. However, halos with this characteristic mass are relatively rare at cosmic dawn. Specifically, a virial mass of $M_{\text{vir}} \sim 10^{8-10} M_{\odot}$ corresponds to a peak height of $\nu \sim 2-3$, where $\nu \equiv \delta_c(z)/\sqrt{S(M_{\text{vir}})}$, with $\delta_c(z)$ denoting the critical linear overdensity for halo formation and $S(M_{\text{vir}})$ the variance of smoothed density field on the mass scale M_{vir} . As we will show shortly, the halos that can undergo core-collapse *in time* to seed BHs are typically of lower mass.

3. THE BH-SEEDING CONDITION

To further clarify the conditions for BH formation via SIDM core-collapse, we compare two key timescales: the core-collapse time, t_{cc} , as defined above, and the *look-back time to the epoch of halo formation*, t_{form} . This comparison is motivated by the fact that gravothermal evolution driven by dark self-interactions only begins after a halo has formed. An SIDM halo is expected to undergo core-collapse and seed a BH if $t_{\text{cc}} < t_{\text{form}}$ — that is, if there is sufficient time since formation for the collapse to occur. We define the halo formation epoch as the cosmic time by which a halo has assembled half of its instantaneous mass², denoted $t_{1/2}$. The look-back time to formation is then

$$t_{\text{form}}(z, M_{\text{vir}}) = t(z) - t_{1/2}(z, M_{\text{vir}}), \quad (7)$$

where $t(z)$ is the cosmic time at redshift z .

The halo-formation time depends on both halo mass and redshift, and can be computed analytically using the extended Press–Schechter (EPS) theory (EPS, e.g., Lacey & Cole 1993). For a halo of mass M_0 at cosmic time t_0 , EPS predicts the ensemble-averaged number of progenitors with mass in the interval $[M_1, M_1 + dM_1]$ at an earlier time t_1 :

$$\frac{dN}{dM_1} dM_1 = \frac{M_0}{M_1} f_{\text{EPS}}(S_1, \delta_1 | S_0, \delta_0) \left| \frac{dS_1}{dM_1} \right| dM_1, \quad (8)$$

where

$$f_{\text{EPS}}(S_1, \delta_1 | S_0, \delta_0) = \sqrt{\frac{1}{2\pi}} \frac{\Delta\delta}{(\Delta S)^{3/2}} \exp\left[-\frac{(\Delta\delta)^2}{2\Delta S}\right], \quad (9)$$

with $\delta = \delta_c(z)$ denoting the linear critical overdensity for halo formation ($\Delta\delta = \delta_1 - \delta_0$), and $S(M)$ the mass

variance of the cosmic density field ($\Delta S = S_1 - S_0$). Because a halo can have at most one progenitor in the mass range $M_1 \in [M_0/2, M_0]$, the probability that a halo formed earlier than time t_1 (i.e., had already assembled at least half its mass by then) is given by:

$$P(< t_1 | M_0, t_0) = \int_{M_0/2}^{M_0} \frac{dN}{dM_1} dM_1. \quad (10)$$

By substituting M_0 with halo mass M_{vir} , t_0 with cosmic time $t(z)$, and t_1 with the formation time $t_{1/2}$, we can differentiate eq. (10) with respect to $t_{1/2}$ to obtain the distribution of halo formation times. This also yields the distribution of the look-back time to halo formation, $t_{\text{form}}(z, M_{\text{vir}})$, which is shown in Fig. 2 as green bands.

In Fig. 2, we compare the look-back time to halo formation, t_{form} , with the core-collapse timescale, t_{cc} , to identify the mass and redshift ranges favorable for BH formation. For illustration, we fix halo concentration at $c = 16$ and the SIDM parameters at $(\sigma_{0m}, \omega) = (30 \text{ cm}^2/\text{g}, \omega = 80 \text{ km/s})$, while scanning halo masses from $M_{\text{vir}} \sim 10^{6.5} M_{\odot}$ to $10^9 M_{\odot}$.

BH formation is not possible if the time since halo formation is insufficient for core-collapse — that is, when $t_{\text{cc}} > t_{\text{form}}$. This region is hatched in Fig. 2, and it encompasses the majority of high-redshift halos. Only a subset of early-forming halos, those in a mass-dependent tail where $t_{\text{cc}} \leq t_{\text{form}}$, can undergo core-collapse in time to seed BHs.

While the specific mass and redshift thresholds depend on the chosen values of halo concentration and cross section, it is clear that this SIDM-based BH seeding mechanism only operates at high redshifts — in this case, $z \gtrsim 8.5$. This is both important and reassuring: if the mechanism remained active at later times, we would expect high occupation fractions of massive BHs in low-mass galaxies, in tension with low-redshift observations (Ho 2008; Kormendy & Ho 2013; Greene et al. 2020).

Another key insight from this analysis is that the BH-seeding mass is lower than the characteristic mass for the most rapid core-collapse. In this example, only halos with $M_{\text{vir}} \sim 10^{6.5-8.5} M_{\odot}$ are able to seed BHs in the redshift range explored, whereas the fastest core-collapse occurs at $\sim 10^9 M_{\odot}$. Assuming a 1% conversion efficiency from halo mass to BH mass (Feng et al. 2021), this implies a seed BH mass range of $M_{\text{bh}} \sim 10^{4.5-6.5} M_{\odot}$. This is an order of magnitude higher than what baryonic seeding mechanisms predict (Li et al. 2023, 2024), but still lower than the BH mass estimates for LRDs, which spans $10^{6-8} M_{\odot}$. Thus, while SIDM core-collapse can naturally produce relatively massive BH seeds, substantial growth is still required to match the observed BH mass distribution.

²We note that this definition is somewhat arbitrary and could be refined through cosmological SIDM simulations that more accurately determine when gravothermal evolution begins. In practice, modelers might consider alternative markers such as the time of the last major merger, or when the halo first assembled the mass enclosed within its instantaneous scale radius r_s .

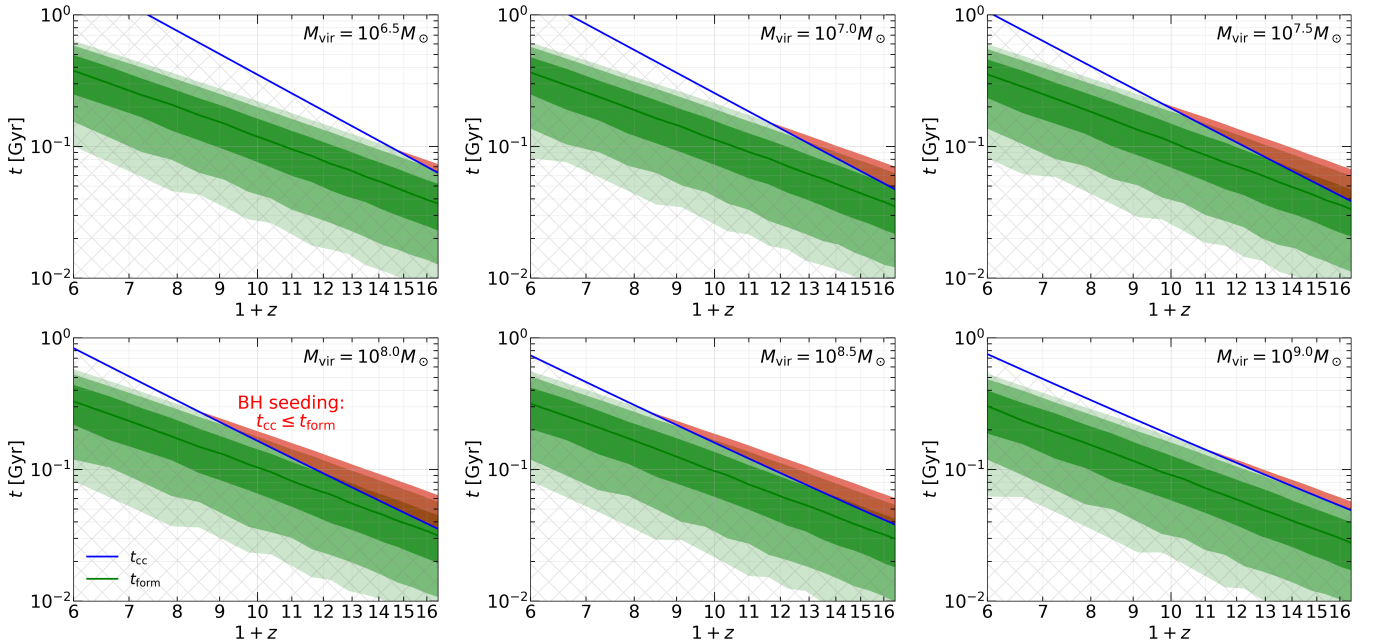


Figure 2. Exploration of the parameter space for BH seeding via core-collapse of SIDM halos, shown as a function of halo mass M_{vir} and redshift z . Each panel corresponds to a different instantaneous halo mass. The halo concentration is fixed at 16. The SIDM cross section is set to be $\sigma_{0m} = 30 \text{ cm}^2/\text{g}$ and $\omega = 80 \text{ km/s}$. Green bands indicate the distribution of look-back times to halo formation, $t_{\text{form}}(z, M_{\text{vir}})$, predicted from the extended Press-Schechter formalism, with different shades representing the 25-75th, 10-90th, and 5-95th percentiles. Blue lines show the core-collapse time $t_{\text{cc}}(z)$, as defined in eq. (3). The hatched regions denote where the time since halo formation is insufficient for core-collapse to occur ($t_{\text{cc}} > t_{\text{form}}$). The early-forming tail, where collapse, and hence BH seeding, is possible ($t_{\text{cc}} \leq t_{\text{form}}$), is highlighted in red. This BH-seeding mechanism operates only at high redshift (in this case, $z \gtrsim 8.5$; the exact threshold depends on concentration and cross section). For seeding to occur within the redshift range explored here, the halo mass must lie in the range $M_{\text{vir}} \sim 10^{7-8.5} M_{\odot}$.

4. SEMI-ANALYTIC MODEL FOR BH SEEDING AND GROWTH

We develop a model for BH seeding and mass growth by incorporating the aforementioned dark-seeding conditions into halo merger trees, along with prescriptions for BH accretion and mergers.

Our first step is to generate cosmological populations of DM halos at early times. This is technically challenging because we focus on the high-concentration, early-forming tail of low-mass halos, with masses as small as $M_{\text{vir}} \sim 10^6 M_{\odot}$. Numerical simulations capable of capturing both the necessary resolution and large cosmic volume would be prohibitively expensive. Therefore, we adopt a semi-analytic approach based on Monte Carlo merger trees and analytical halo mass functions (HMFs).

Specifically, we construct merger trees using the algorithm of Parkinson et al. (2008), as implemented in the semi-analytic framework **SatGen** (Jiang et al. 2021), which has been shown to produce merger statistics consistent with cosmological simulations (Jiang & van den Bosch 2014). We select a final redshift of $z = 5$ and generate N_i merger trees for final halo masses $M_{\text{vir},i} = 10^{8, 8.25, 8.5, \dots, 11.5} M_{\odot}$. The number of trees N_i is set to 32 for the most massive final halos, and increases to-

wards lower masses in proportion to the HMF at $z = 5$, as computed using the **hmf** calculator (Murray et al. 2013). For each progenitor halo in the merger trees, we trace the full formation history (i.e., all branches) down to a resolution mass of $M_{\text{res}} = 10^6 M_{\odot}$. To ensure accurate tracking of halo formation times, we further extend the main branch near this resolution limit down to a *leaf* mass of $10^4 M_{\odot}$. The resulting merger trees provide the virial masses of all progenitor halos, $M_{\text{vir}}(z)$, at $z > 5$, enabling us to evaluate when and where BH seeding can occur.

Second, we assign a concentration parameter c to each progenitor branch. To do so, we measure the distribution of halo concentrations in the high-resolution cosmological simulation, **VVV-L1** (Wang et al. 2020), applying the method of Wang et al. (2024) to all well-resolved, relaxed halos³. We find that the distribution

³We consider a halo *relaxed* if its substructure fraction is less than 0.1 and the offset between its gravitational-potential minimum and its center-of-mass is less than $0.07 r_{\text{vir}}$ (Neto et al. 2007). We consider a halo *well-resolved* if it has more than 100 particles, and with the Wang et al. (2024) method, we are able to achieve concentration convergence within 10% for such halos.

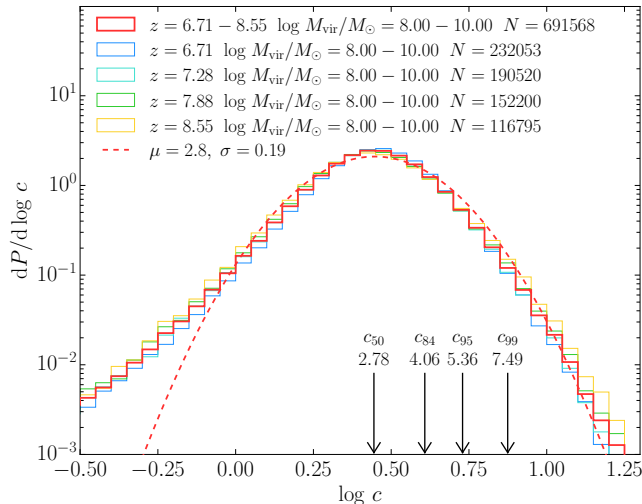


Figure 3. The distribution of halo concentration c in the early Universe, measured from the VV-L1 cosmological simulation (Wang et al. 2020). No significant redshift dependence is observed across the redshift range. We also find minimal mass dependence over the simulation’s mass range of $10^{8-10} M_{\odot}$. The arrows mark the 50th, 84th, 95th, and 99th percentiles of the full distribution. The high- c tail is well described by a log-normal distribution with a median $c = 2.8$ and a scatter $\sigma_{\log(c)} \approx 0.19$. We sample from this distribution to assign concentrations to progenitor halos in the merger trees (see text).

of c shows negligible dependence on redshift at high z , as illustrated in Fig. 3, and almost no dependence on halo mass either (not shown here). The high- c tail is well described by a log-normal distribution with a median $c = 2.8$ and a scatter of $\sigma_{\log c} \approx 0.19$. Although the distribution features an extended low- c tail, we do not attempt to model this regime accurately since halos with such low concentrations are incapable of undergoing core-collapse. Therefore, for each progenitor branch in the merger trees, we draw a concentration value c from this log-normal distribution. We assume c to be constant along a progenitor branch, assigning it once per branch. While this is a simplification, it reasonably captures the expectation that halo concentration evolves slowly in the absence of major mergers.

Third, with halo masses $M_{\text{vir}}(z)$ provided by the merger trees and concentrations c drawn from the empirical distribution shown in Fig. 3, we compute the core-collapse time t_{cc} using eq. (3). The merger trees also supply the look-back time to halo formation, $t_{\text{form}}(z)$, for each progenitor. For a halo with mass $M_{\text{vir}}(z)$ and concentration c , if the condition $t_{\text{cc}}[M_{\text{vir}}(z), c] < t_{\text{form}}(z)$ is satisfied, we assume that the halo has undergone core-collapse and seeded a BH. In that case, we assign a BH seed with mass $M_{\text{bh}} = 0.01 M_{\text{vir}}$ to the halo

and track its subsequent mass growth, as described below. To enhance statistics, for each of the merger trees, we have 10 Monte Carlo realizations of BH seeding.

Finally, we consider BH mass growth and mergers. The BH growth rate is given by (Loeb & Furlanetto 2013):

$$\dot{M}_{\text{bh}} = M_{\text{bh}}/t_{\text{E}}, \quad (11)$$

where the e-folding times for BH growth, t_{E} , is given by

$$t_{\text{E}} = 0.45 \text{ Gyr } \epsilon / (1 - \epsilon) \lambda_{\text{E}}^{-1}, \quad (12)$$

with λ_{E} being the Eddington ratio and ϵ the radiative efficiency, typically assumed to be 0.1 (Shakura & Sunyaev 1976). For simplicity, we draw λ_{E} from a log-normal distribution (Willott et al. 2010; Xiao et al. 2021), with a median of 0.2 and a scatter of $\sigma_{\log \lambda_{\text{E}}} = 0.3$. We emphasize that these choices are intended for proof-of-concept purposes, and the values are not necessarily what we advocate.

When two BH-hosting halos merge, we assume the BHs coalesce after a delay set by the dynamical-friction timescale (Boylan-Kolchin et al. 2008):

$$t_{\text{merge}} = 0.216 \frac{(M_{\text{vir}}/m_{\text{vir}})^{1.3}}{\ln(1 + M_{\text{vir}}/m_{\text{vir}})} e^{1.9\eta} x_{\text{circ}} t_{\text{cross}} \quad (13)$$

where η is orbital circularity, x_{circ} characterizes the orbital energy, and $t_{\text{cross}} = \sqrt{3/(4\pi G \Delta \rho_{\text{crit}})}$ is the virial crossing time. We adopt typical values from cosmological simulations, fixing $\eta = 0.5$ and $x_{\text{circ}} = 1$ (Zentner et al. 2005).

5. THE BH MASS FUNCTION FOR LITTLE RED DOTS

Using this model, we generate random realizations of halo merger trees, populate the halos that satisfy the core-collapse condition with BH seeds, and evolve their masses over time. We have verified that the resulting halo populations are cosmologically representative by confirming that the distribution of $M_{\text{vir}}(z)$ at high redshifts agrees with the theoretical HMFs at those epochs, as computed using the `hmf` tool.

Through trial and error, we find that an SIDM cross section characterized by $\sigma_{0m} = 30 \text{ cm}^2/\text{g}$ and $\omega = 80 \text{ km/s}$ yields BH mass functions in good agreement with those observationally inferred for LRDs. The comparison is shown in Fig. 4, where we adopt observational benchmarks from Kokorev et al. (2024, see their Table 2 and Fig.6) for LRDs at $z \approx 4.5-6.5$, and compute the model predictions at a comparable redshift of $z = 5$. We emphasize that our model is not a fit to the data,

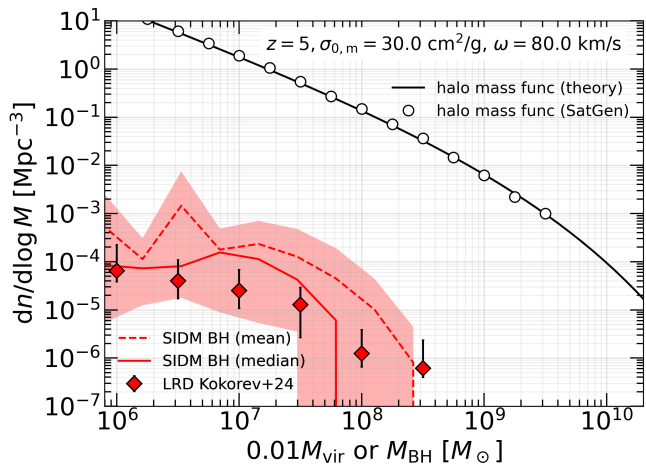


Figure 4. BH mass function at $z = 5$ predicted by the model of SIDM core-collapse and BH growth. The SIDM cross section is set to $\sigma_{0m} = 30 \text{ cm}^2/\text{g}$ and $\omega = 80 \text{ km/s}$. The red solid and dashed lines show the median and mean BH mass functions, respectively, from random model realizations (see Section 4). The red shaded region indicates the full scatter across these realizations. Observationally inferred BH mass functions for LRDs at $z = 4.5\text{--}6.5$ are shown as diamonds with error bars, adopted from Kokorev et al. (2024). The open circles represent the HMF from our model realizations, which is in good agreement with the theoretical value from `hmf`.

and the adopted cross-section parameters should not be interpreted as the best-fit or preferred values. Several nuisance parameters — such as the Eddington ratio and the mass fraction of a core-collapsed halo converted into a BH — can significantly affect the BH mass function. However, variations in these parameters primarily shift the model predictions horizontally in Fig. 4, rather than altering the overall shape or normalization. To obtain the exact halo-mass fraction of a BH seed requires a relativistic version of gravothermal evolution (Shapiro 2018), and will be explored in a future study (Feng et al., in prep). We also neglect the contribution from baryonic BH seeding mechanisms in this work.

A full marginalization over nuisance parameters to constrain the SIDM cross section is beyond the scope of this study and is technically challenging. This is largely due to the computational cost of generating statistically meaningful samples of BHs, given their extremely low occupation numbers in halos. This rarity is already apparent from the > 4 dex gap between the halo mass function and the BH mass function in Fig. 4, and the challenge becomes even more severe for smaller cross sections. That said, we have verified that the normalization of the BH mass function is highly sensitive to the cross section. For example, not shown here, increasing σ_{0m} by a factor of 2 leads to BH mass functions that over-

shoot observational estimates by more than an order of magnitude.

6. DISCUSSION

SIDM is a popular framework in near-field cosmology, especially in addressing the structures of dwarf halos (Spergel & Steinhardt 2000; Vogelsberger et al. 2012; Creasey et al. 2017; Roberts et al. 2024) and statistics of satellite galaxies (Vogelsberger et al. 2019; Zeng et al. 2022; O’Neil et al. 2023). Constraints on SIDM cross-section parameters are primarily derived from DM density profiles inferred through galaxy kinematic observations (e.g., Slone et al. 2023; Yang et al. 2024; Ando et al. 2025). Despite recent progress, relatively broad regions of the parameter space remain viable. For instance, both small, nearly constant cross sections ($\sigma_{0m} \sim 1 \text{ cm}^2/\text{g}$, $\omega \gtrsim 100 \text{ km/s}$) and large cross sections at low-velocities ($\sigma_{0m} \gtrsim 100 \text{ cm}^2/\text{g}$, $\omega \sim 10\text{--}100 \text{ km/s}$) can successfully reproduce galaxy rotation curves (RCs).

Particular attention has recently been drawn to the strongly interacting regime, broadly characterized by an effective cross section of $\sim 20\text{--}40 \text{ cm}^2/\text{g}$ (Roberts et al. 2024). This regime is especially attractive because such cross sections can lead to either cuspy or cored profiles, depending on the formation time and the initial halo concentration — offering a natural explanation for the observed structural diversity in dwarf galaxies. In fact, Turner et al. (2021) and Yang et al. (2023) explore even stronger interactions, using cross sections as large as $\sigma_m \sim 100 \text{ cm}^2/\text{g}$ at $v \sim 10 \text{ km/s}$, and report reasonable agreement between their SIDM simulations and Milky Way satellites.

In a companion study (Jia et al., in prep.), we refine the model for computing SIDM density profiles (Jiang et al. 2023; Yang et al. 2024) based on the isothermal Jeans framework (Kaplinghat et al. 2014, 2016). By incorporating the effects of adiabatic contraction and a prescription for the early stages of core-collapse, we are able to utilize a much larger fraction of the SPARC galaxy sample, including those with baryon-dominated centers — unlike many earlier studies which excluded such systems. The resulting constraints on the SIDM cross section form a degenerate stripe in parameter space, as shown in Fig. 5, where the blue band of low reduced χ^2 from RC fitting highlights the region favored by this analysis. These constraints are consistent with other recent estimates of SIDM cross sections (e.g., Ando et al. 2025). Interestingly, the cross-section parameters we explore in this work, $\sigma_{0m} = 30 \text{ cm}^2/\text{g}$ and $\omega = 80 \text{ km/s}$, fall squarely within this preferred region. Although we emphasize that these values were not tuned to match the data, this coincidence is encourag-

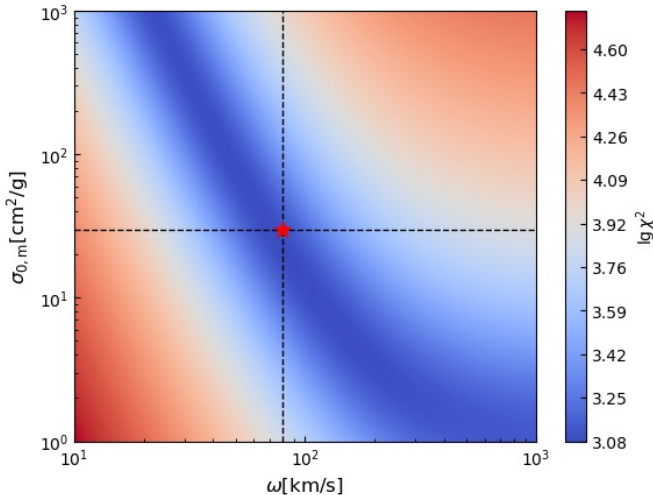


Figure 5. Constraints on the SIDM cross section from the local Universe, based on galaxy rotation curve (RC) fitting, adapted from Jia et al. (in prep). The color scale indicates the reduced χ^2 from fitting RCs in the SPARC survey (Lelli et al. 2016), using SIDM halo profiles derived from an improved version (Jiang et al. 2023) of the isothermal Jeans model (Kaplinghat et al. 2014). The SIDM cross-section parameters adopted in Fig. 4 — which successfully reproduce the observed BH mass functions of LRDs — fall within the region independently favored by these local RC constraints.

ing. It suggests that statistics of high-redshift BHs may provide an independent and complementary avenue for constraining SIDM cross sections — one that is orthogonal to traditional approaches based on local galaxy kinematics.

7. CONCLUSION

In this Letter, we explored the feasibility of seeding *massive* and *naked* BHs observed in LRDs through gravothermal core-collapse in SIDM halos, using a statistical, semi-analytical framework. We characterized the properties of BH-seeding halos in terms of their concentration, mass, and formation redshift, and found that they must form early (at $z \gtrsim 8.5$), be highly concentrated ($c \gtrsim 10$), and reside within a specific mass range ($M_{\text{vir}} \sim 10^{6.5-8.5} M_{\odot}$) in order to seed BHs at the right times (during or slightly before re-ionization).

The required high concentrations arise naturally and ubiquitously at early times in standard cosmological models, as confirmed by high-resolution simulations of early halos (Wang et al. 2020). The concentration distribution exhibits a median value of $c = 2.8$ with a log-

normal high- c tail extending to $c \gtrsim 10$, largely independent of halo mass and redshift. While the precise seeding conditions depend on the SIDM cross section, the qualitative behavior is appealing: the dark-seeding mechanism activates only at cosmic dawn, and the resulting BH seed masses naturally fall close to the expected range for LRDs, assuming a $\sim 1\%$ BH-to-halo mass ratio (Feng et al. 2021).

As a proof of concept, we showed that a modestly high SIDM cross section — $\sigma_{0m} = 30 \text{ cm}^2/\text{g}$ and $\omega = 80 \text{ km/s}$ — yields BH mass functions in good agreement with those inferred from LRD observations. Remarkably, this parameter choice also lies within the region independently favored by SIDM constraints based on the rotation curves of nearby galaxies.

Although our analysis is framed in the context of LRDs, we emphasize that the results represent a general prediction of the SIDM paradigm. Previous studies have extensively studied SIDM core-collapse since the early work of Balberg & Shapiro (2002). Our contribution here takes a further step, demonstrating that within this DM framework, the formation of a cosmologically significant population of massive BHs at cosmic dawn is not only plausible — it is inevitable.

We have presented a theoretical framework to characterize this population and advocate for its inclusion in future SIDM studies. Incorporating high- z BH statistics alongside local galaxy kinematics could lead to joint constraints on the particle properties of DM. Given SIDM’s compelling ability to explain the structural diversity of dwarf galaxies, we argue that it must be taken seriously as a viable, non-baryonic channel for BH seeding.

- 1 FJ thanks Haibo Yu, Daneng Yang, and Joel Primack
- 2 for helpful discussions. FJ, ZJ, and this work is sup-
- 3 ported by the National Science Foundation of China
- 4 (NSFC, 12473007) and the Beijing Natural Science
- 5 Foundation (2401113911). LCH acknowledges support
- 6 by the NSFC (12233001) and the National Key R&D
- 7 Program of China (2022YFF0503401). KI acknowl-
- 8 edges support from the NSFC (12073003, 11721303,
- 9 11991052, 12233001), the National Key R&D Program
- 10 of China (2022YFF0503401), and the China Manned
- 11 Space Project (CMS-CSST-2021-A04 and CMS-CSST-
- 12 2021-A06). WXF acknowledges support from China
- 13 Postdoctoral Science Foundation (2024M761594).

REFERENCES

Ando, S., Hayashi, K., Horigome, S., Ibe, M., & Shirai, S. 2025, arXiv

Balberg, S., & Shapiro, S. L. 2002, Physical Review Letters, 88, 101301, doi: [10.1103/physrevlett.88.101301](https://doi.org/10.1103/physrevlett.88.101301)

- Boylan-Kolchin, M., Ma, C.-P., & Quataert, E. 2008, *Monthly Notices of the Royal Astronomical Society*, 383, 93, doi: [10.1111/j.1365-2966.2007.12530.x](https://doi.org/10.1111/j.1365-2966.2007.12530.x)
- Chen, C.-H., Ho, L. C., Li, R., & Zhuang, M.-Y. 2024, arXiv, doi: [10.48550/arXiv.2411.04446](https://doi.org/10.48550/arXiv.2411.04446)
- Creasey, P., Sameie, O., Sales, L. V., et al. 2017, *Monthly Notices of the Royal Astronomical Society*, 468, 2283, doi: [10.1093/mnras/stx522](https://doi.org/10.1093/mnras/stx522)
- Despali, G., Moscardini, L., Nelson, D., et al. 2025, arXiv, doi: [10.48550/arXiv.2501.12439](https://doi.org/10.48550/arXiv.2501.12439)
- Essig, R., McDermott, S. D., Yu, H.-B., & Zhong, Y.-M. 2019, *Physical Review Letters*, 123, 121102, doi: [10.1103/physrevlett.123.121102](https://doi.org/10.1103/physrevlett.123.121102)
- Feng, W.-X., Yu, H.-B., & Zhong, Y.-M. 2021, *The Astrophysical Journal Letters*, 914, L26, doi: [10.3847/2041-8213/ac04b0](https://doi.org/10.3847/2041-8213/ac04b0)
- . 2022, *Journal of Cosmology and Astroparticle Physics*, 2022, 036, doi: [10.1088/1475-7516/2022/05/036](https://doi.org/10.1088/1475-7516/2022/05/036)
- Greene, J. E., Strader, J., & Ho, L. C. 2020, *Annual Review of Astronomy and Astrophysics*, 58, 1, doi: [10.1146/annurev-astro-032620-021835](https://doi.org/10.1146/annurev-astro-032620-021835)
- Greene, J. E., Labbe, I., Goulding, A. D., et al. 2024, *The Astrophysical Journal*, 964, 39, doi: [10.3847/1538-4357/ad1e5f](https://doi.org/10.3847/1538-4357/ad1e5f)
- Ho, L. C. 2008, *Annual Review of Astronomy and Astrophysics*, 46, 475, doi: [10.1146/annurev.astro.45.051806.110546](https://doi.org/10.1146/annurev.astro.45.051806.110546)
- Inayoshi, K., Visbal, E., & Haiman, Z. 2020, *Annual Review of Astronomy and Astrophysics*, 58, 1, doi: [10.1146/annurev-astro-120419-014455](https://doi.org/10.1146/annurev-astro-120419-014455)
- Jiang, F., Dekel, A., Freundlich, J., et al. 2021, *Monthly Notices of the Royal Astronomical Society*, 502, 621, doi: [10.1093/mnras/staa4034](https://doi.org/10.1093/mnras/staa4034)
- Jiang, F., & van den Bosch, F. C. 2014, *Monthly Notices of the Royal Astronomical Society*, 440, 193, doi: [10.1093/mnras/stu280](https://doi.org/10.1093/mnras/stu280)
- Jiang, F., Benson, A., Hopkins, P. F., et al. 2023, *Monthly Notices of the Royal Astronomical Society*, doi: [10.1093/mnras/stad705](https://doi.org/10.1093/mnras/stad705)
- Kaplinghat, M., Keeley, R. E., Linden, T., & Yu, H.-B. 2014, *Physical Review Letters*, 113, 021302, doi: [10.1103/physrevlett.113.021302](https://doi.org/10.1103/physrevlett.113.021302)
- Kaplinghat, M., Tulin, S., & Yu, H.-B. 2016, *Physical Review Letters*, 116, 041302, doi: [10.1103/physrevlett.116.041302](https://doi.org/10.1103/physrevlett.116.041302)
- Kocevski, D. D., Finkelstein, S. L., Barro, G., et al. 2024, arXiv, doi: [10.48550/arXiv.2404.03576](https://doi.org/10.48550/arXiv.2404.03576)
- Kokorev, V., Caputi, K. I., Greene, J. E., et al. 2024, *The Astrophysical Journal*, 968, 38, doi: [10.3847/1538-4357/ad4265](https://doi.org/10.3847/1538-4357/ad4265)
- Kormendy, J., & Ho, L. C. 2013, *Annual Review of Astronomy and Astrophysics*, 51, 511, doi: [10.1146/annurev-astro-082708-101811](https://doi.org/10.1146/annurev-astro-082708-101811)
- Lacey, C., & Cole, S. 1993, *Monthly Notices of the Royal Astronomical Society* (ISSN 0035-8711), 262, 627, doi: [10.1093/mnras/262.3.627](https://doi.org/10.1093/mnras/262.3.627)
- Lelli, F., McGaugh, S. S., & Schombert, J. M. 2016, *The Astrophysical Journal*, 152, 157, doi: [10.3847/0004-6256/152/6/157](https://doi.org/10.3847/0004-6256/152/6/157)
- Li, W., Inayoshi, K., Onoue, M., & Toyouchi, D. 2023, *The Astrophysical Journal*, 950, 85, doi: [10.3847/1538-4357/acbbe](https://doi.org/10.3847/1538-4357/acbbe)
- Li, W., Inayoshi, K., Onoue, M., et al. 2024, *The Astrophysical Journal*, 969, 69, doi: [10.3847/1538-4357/ad46f9](https://doi.org/10.3847/1538-4357/ad46f9)
- Loeb, A., & Furlanetto, S. R. 2013, *The First Galaxies in the Universe* (Princeton University Press)
- Maiolino, R., Scholtz, J., Curtis-Lake, E., et al. 2024, *Astronomy & Astrophysics*, 691, A145, doi: [10.1051/0004-6361/202347640](https://doi.org/10.1051/0004-6361/202347640)
- Matthee, J., Naidu, R. P., Brammer, G., et al. 2024, *The Astrophysical Journal*, 963, 129, doi: [10.3847/1538-4357/ad2345](https://doi.org/10.3847/1538-4357/ad2345)
- Murray, S., Power, C., & Robotham, A. 2013, *Astronomy and Computing*, 3, 23, doi: [10.1016/j.ascom.2013.11.001](https://doi.org/10.1016/j.ascom.2013.11.001)
- Navarro, J. F., Frenk, C. S., & White, S. D. M. 1997, *The Astrophysical Journal*, 490, 493, doi: [10.1086/304888](https://doi.org/10.1086/304888)
- Neto, A. F., Gao, L., Bett, P., et al. 2007, *Monthly Notices of the Royal Astronomical Society*, 381, 1450, doi: [10.1111/j.1365-2966.2007.12381.x](https://doi.org/10.1111/j.1365-2966.2007.12381.x)
- Nishikawa, H., Boddy, K. K., & Kaplinghat, M. 2020, *Physical Review D*, 101, 063009, doi: [10.1103/physrevd.101.063009](https://doi.org/10.1103/physrevd.101.063009)
- O'Neil, S., Vogelsberger, M., Heeba, S., et al. 2023, *Monthly Notices of the Royal Astronomical Society*, 524, 288, doi: [10.1093/mnras/stad1850](https://doi.org/10.1093/mnras/stad1850)
- Parkinson, H., Cole, S., & Helly, J. 2008, *Monthly Notices of the Royal Astronomical Society*, 383, 557, doi: [10.1111/j.1365-2966.2007.12517.x](https://doi.org/10.1111/j.1365-2966.2007.12517.x)
- Pollack, J., Spergel, D. N., & Steinhardt, P. J. 2015, *The Astrophysical Journal*, 804, 131, doi: [10.1088/0004-637x/804/2/131](https://doi.org/10.1088/0004-637x/804/2/131)
- Reines, A. E., & Volonteri, M. 2015, *The Astrophysical Journal*, 813, 82, doi: [10.1088/0004-637X/813/2/82](https://doi.org/10.1088/0004-637X/813/2/82)
- Roberts, M. G., Braff, L., Garg, A., et al. 2025, *Journal of Cosmology and Astroparticle Physics*, 2025, 060, doi: [10.1088/1475-7516/2025/01/060](https://doi.org/10.1088/1475-7516/2025/01/060)
- Roberts, M. G., Kaplinghat, M., Valli, M., & Yu, H.-B. 2024, arXiv, doi: [10.48550/arXiv.2407.15005](https://doi.org/10.48550/arXiv.2407.15005)

- Rocha, M., Peter, A. H. G., Bullock, J. S., et al. 2013, *Monthly Notices of the Royal Astronomical Society*, 430, 81, doi: [10.1093/mnras/sts514](https://doi.org/10.1093/mnras/sts514)
- Sales, L. V., Wetzel, A., & Fattahi, A. 2022, *Nature Astronomy*, 6, 897, doi: [10.1038/s41550-022-01689-w](https://doi.org/10.1038/s41550-022-01689-w)
- Shakura, N. I., & Sunyaev, R. A. 1976, *Monthly Notices of the Royal Astronomical Society*, 175, 613, doi: [10.1093/mnras/175.3.613](https://doi.org/10.1093/mnras/175.3.613)
- Shapiro, S. L. 2018, *Physical Review D*, 98, 023021, doi: [10.1103/PhysRevD.98.023021](https://doi.org/10.1103/PhysRevD.98.023021)
- Slone, O., Jiang, F., Lisanti, M., & Kaplinghat, M. 2023, *Physical Review D*, 107, 043014, doi: [10.1103/PhysRevD.107.043014](https://doi.org/10.1103/PhysRevD.107.043014)
- Spiegel, D. N., & Steinhardt, P. J. 2000, *Physical Review Letters*, 84, 3760, doi: [10.1103/PhysRevLett.84.3760](https://doi.org/10.1103/PhysRevLett.84.3760)
- Taylor, A. J., Finkelstein, S. L., Kocevski, D. D., et al. 2024, arXiv, doi: [10.48550/arXiv.2409.06772](https://doi.org/10.48550/arXiv.2409.06772)
- Turner, H. C., Lovell, M. R., Zavala, J., & Vogelsberger, M. 2021, *Monthly Notices of the Royal Astronomical Society*, 505, 5327, doi: [10.1093/mnras/stab1725](https://doi.org/10.1093/mnras/stab1725)
- Vogelsberger, M., Zavala, J., & Loeb, A. 2012, *Monthly Notices of the Royal Astronomical Society*, 423, 3740, doi: [10.1111/j.1365-2966.2012.21182.x](https://doi.org/10.1111/j.1365-2966.2012.21182.x)
- Vogelsberger, M., Zavala, J., Schutz, K., & Slatyer, T. R. 2019, *Monthly Notices of the Royal Astronomical Society*, 484, 5437, doi: [10.1093/mnras/stz340](https://doi.org/10.1093/mnras/stz340)
- Volonteri, M., Habouzit, M., & Colpi, M. 2021, *Nature Reviews Physics*, 3, 732, doi: [10.1038/s42254-021-00364-9](https://doi.org/10.1038/s42254-021-00364-9)
- Wang, J., Bose, S., Frenk, C. S., et al. 2020, *Nature*, 585, 39, doi: [10.1038/s41586-020-2642-9](https://doi.org/10.1038/s41586-020-2642-9)
- Wang, K., Mo, H. J., Chen, Y., & Schaye, J. 2024, *MNRAS*, 527, 10760, doi: [10.1093/mnras/stad3927](https://doi.org/10.1093/mnras/stad3927)
- Weinberg, D. H., Bullock, J. S., Governato, F., Naray, R. K. d., & Peter, A. H. G. 2015, *Proceedings of the National Academy of Sciences*, 112, 12249, doi: [10.1073/pnas.1308716112](https://doi.org/10.1073/pnas.1308716112)
- Willott, C. J., Albert, L., Arzoumanian, D., et al. 2010, *The Astronomical Journal*, 140, 546, doi: [10.1088/0004-6256/140/2/546](https://doi.org/10.1088/0004-6256/140/2/546)
- Xiao, H., Shen, X., Hopkins, P. F., & Zurek, K. M. 2021, *Journal of Cosmology and Astroparticle Physics*, 2021, 039, doi: [10.1088/1475-7516/2021/07/039](https://doi.org/10.1088/1475-7516/2021/07/039)
- Yang, D., Nadler, E. O., & Yu, H.-B. 2023, *The Astrophysical Journal*, 949, 67, doi: [10.3847/1538-4357/acc73e](https://doi.org/10.3847/1538-4357/acc73e)
- Yang, D., & Yu, H.-B. 2022, *Journal of Cosmology and Astroparticle Physics*, 2022, 077, doi: [10.1088/1475-7516/2022/09/077](https://doi.org/10.1088/1475-7516/2022/09/077)
- Yang, S., Jiang, F., Benson, A., et al. 2024, *Monthly Notices of the Royal Astronomical Society*, 533, 4007, doi: [10.1093/mnras/stae2038](https://doi.org/10.1093/mnras/stae2038)
- Yung, L. Y. A., Somerville, R. S., Nguyen, T., et al. 2024, *Monthly Notices of the Royal Astronomical Society*, 530, 4868, doi: [10.1093/mnras/stae1188](https://doi.org/10.1093/mnras/stae1188)
- Zeng, Z. C., Peter, A. H. G., Du, X., et al. 2022, *Monthly Notices of the Royal Astronomical Society*, 513, 4845, doi: [10.1093/mnras/stac1094](https://doi.org/10.1093/mnras/stac1094)
- Zentner, A. R., Kravtsov, A. V., Gnedin, O. Y., & Klypin, A. A. 2005, *The Astrophysical Journal*, 219, doi: [10.1086/431355](https://doi.org/10.1086/431355)